Fish and Shellfish Immunology 136 (2023) 108706

Contents lists available at ScienceDirect

Fish and Shellfish Immunology

journal homepage: www.elsevier.com/locate/fsi

Full length article

ATG16L1 negatively regulates MAVS-mediated antiviral signaling in black carp *Mylopharyngodon piceus*

Yunfan He [1], Yuqing Peng [1], Xiaoyu Liu, Jiamin Yu, Yuting Du, Zhiming Li, Hui Wu, Jun Xiao [*], Hao Feng [**]

State Key Laboratory of Developmental Biology of Freshwater Fish, College of Life Science, Hunan Normal University, Changsha, 410081, China

ARTICLE INFO

Keywords:
Black carp
ATG16L1
MAVS
IFN

ABSTRACT

Autophagy related 16 like 1 (ATG16L1) is a crucial component of autophagy that regulates the formation of the autophagosome. In mammals, ATG16L1 also performs important roles in immunity, including controlling viral replication and regulating innate immune signaling; however, investigation on the role of piscine ATG16L1 in immunity is rare. In this report, the ATG16L1 homolog of black carp *Mylopharyngodon piceus* (bcATG16L1) was cloned and identified, and its negative regulatory role in mitochondrial antiviral signaling protein (MAVS)-mediated antiviral signaling was described. The coding region of bcATG16L1 consists of 1830 nucleotides and encodes 609 amino acids, including one coiled-coil domain at the N-terminus, three low complexity region domains in the middle, and seven WD40 domains at the C-terminus. By immunofluorescence assay and immunoblotting, we found that bcATG16L1 is a cytosolic protein with a molecular weight of ~74 kDa. In addition, over-expression of bcATG16L1 suppressed bcMAVS-mediated bcIFNa and DrIFNφ1 promoters transcriptional activity and inhibited bcMAVS-mediated antiviral activity. We further confirmed the co-localization of bcATG16L1 and bcMAVS by immunofluorescence assay and verified the protein interaction between bcATG16L1 and bcMAVS by immunoprecipitation assay. Our results report for the first time that black carp ATG16L1 suppresses MAVS-mediated antiviral signaling in teleost fish.

1. Introduction

The innate immune response, which serves as the initial line of defense for the host, is rapidly triggered upon recognition of invading pathogens such as viruses [1]. RIG-I-like receptors (RLRs), including retinoic acid inducible gene I (RIG-I), melanoma differentiation-associated protein 5 (MDA5), and laboratory of genetics and physiology 2 (LGP2), are the major cytoplasmic receptors that recognize RNA viruses and meditate intracellular antiviral response [2]. Mitochondrial antiviral signaling protein (MAVS) is the key adaptor protein in RLR signaling pathway. When the cytosolic helicases such as RIG-I and MDA5 sense viral dsRNAs, they will bind to and activate MAVS through their CARD domains. This contact causes MAVS to oligomerize on the surface of the mitochondria and further recruit downstream protein kinases such as TANK-binding kinase 1 (TBK1). Subsequently, these kinases phosphorylate the interferon regulatory factors (IRFs), which leads to the synthesis of type I interferons (IFNs) [3,4].

Autophagy is an evolutionarily conserved process allowing the orderly degradation and recycling of cellular components [5]. Studies have revealed that autophagy is involved in the regulation of many kinds of life activities such as aging [6,7], neurological diseases [8], cardiovascular diseases [9], and cancer [10]. Accumulating evidence has shown that autophagy also plays an important role in antiviral innate immunity, which may directly affect the life cycle of viruses in cells or modulate antiviral type I IFN signal transduction. For instance, autophagy can stop the spread of viruses by compartmentalizing and destroying their products. However, autophagy is also used by a number of viruses for their proper reproduction.

Autophagy begins with the *de novo* development of the

* Corresponding author. State Key Laboratory of Developmental Biology of Freshwater Fish, College of Life Science, Hunan Normal University, Changsha, 410000, China.

** Corresponding author. State Key Laboratory of Developmental Biology of Freshwater Fish, College of Life Science, Hunan Normal University, Changsha, 410000, China.

E-mail addresses: xiaojun@hunnu.edu.cn (J. Xiao), fenghao@hunnu.edu.cn (H. Feng).

[1] These authors contributed equally to this paper.

https://doi.org/10.1016/j.fsi.2023.108706
Received 27 November 2022; Received in revised form 21 February 2023; Accepted 22 March 2023
Available online 23 March 2023
1050-4648/© 2023 Elsevier Ltd. All rights reserved.

Table 1
Primers used in the study.

Primer name	Sequence (5′-3′)	Primer information
CDS		
bcATG16L1-F	ATGGCTGGACGTGGAGTC	For bcATG16L1 CDS cloning
bcATG16L1-R	CATGTCAGACCAAAGCAC	
Expression construct		
bcATG16L1-F(N)	ACTGACGGTACCGCCACCATGGCTGGACGTGGAGTC	For plasmid construction
bcATG16L1-R(N)	ACTGACCTCGAGCATGTCAGACCAAAGCAC	
q-PCR		
bc Q actin-F	TGGGCACCGCTGCTTCCT	q-PCR
bc Q actin-R	TGTCCGTCAGGCAGCTCAT	q-PCR
SVCV(M)-F	GCCAAATGCCTCCTT	q-PCR
SVCV(M)-R	AGCCCGACCTCCTCTA	q-PCR
SVCV(N)–F	TCTTCTTGCTGGGTCT	q-PCR
SVCV(N)-R	TTGTGAGTTGCCGTTA	q-PCR
SVCV(P)–F	GAGAAAGTAGCAGCATC	q-PCR
SVCV(P)-R	ACTATCCCAGGTCCAA	q-PCR
SVCV(G)-F	ACTATCCCAGGTCCAA	q-PCR
SVCV(G)-R	TGAGGGATAATATCGGCTTG	q-PCR

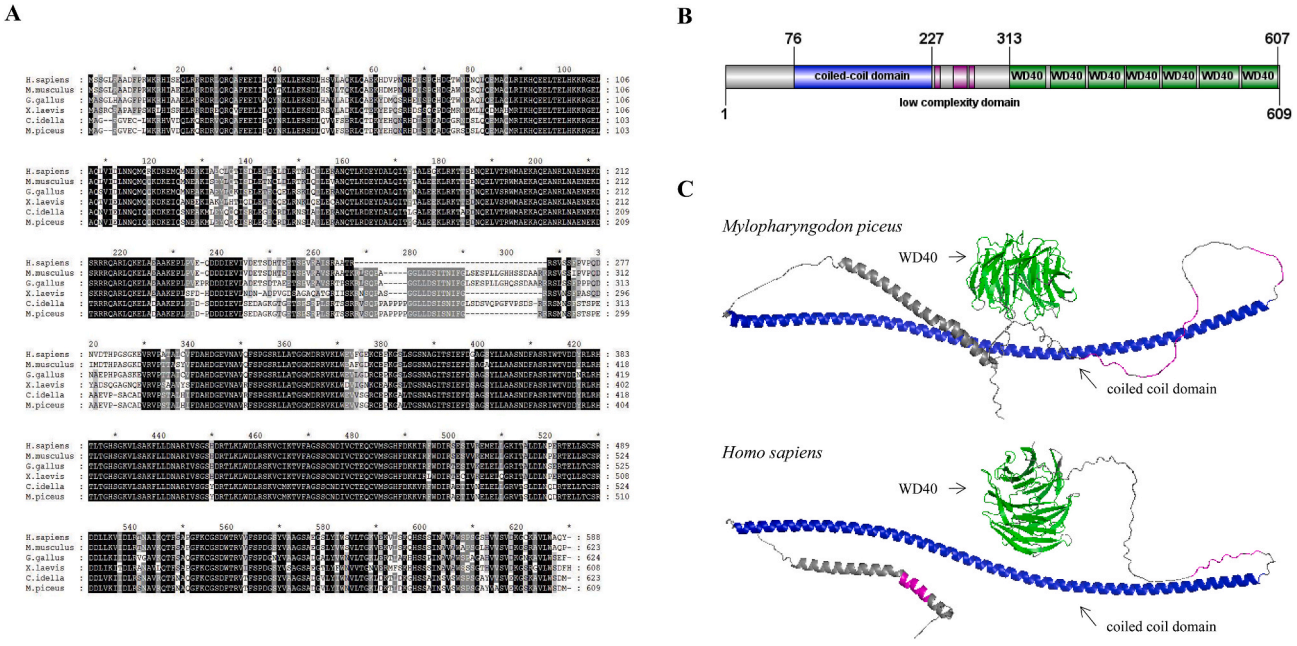

Fig. 1. Sequence analysis of bcATG16L1.
(A) Amino acid sequence alignment of bcATG16L1 with its homologs in *Homo sapiens* (NP_060444.3), *Mus musculus* (NP_001192320.1), *Gallus gallus* (XP_004936995.1), *Xenopus laevis* (XP_018119680.1) and *Ctenopharyngodon idella* (QEE80076.1) by using MEGA-X program and GeneDoc program. (B) Protein structure domain of bcATG16L1. The diagram was made by using Illustrator for Biological Sequences (IBS). (C) Prediction of bcATG16L1 protein 3D structure. The domain prediction results of figures B and C are both predicted by SMART (http://smart.embl.de/).

autophagosome, a double-membrane vesicle that engulfs cellular material and transports it to the lysosome for destruction [11]. This process is precisely regulated by a series of autophagy-related genes (ATGs). ATG16L1 (autophagy related 16 like 1) is a conserved autophagy-related protein in ATG12-ATG5-ATG16 and LC3-PE systems. It participates in mediating the recruitment of the ATG5-ATG12 complex to the phagosome during autophagic vesicle formation and encourages phagosome growth by localizing to endocytic vesicles [12,13]. In addition to canonical autophagy, ATG16L1 is also involved in non-canonical autophagy. Non-canonical autophagy is a key cellular pathway of immunity [14]. In a recent study, the WD40 domain of ATG16L1 interacts with V-ATPase, which may be necessary for the conjugation of Atg8-family proteins to single membranes in non-canonical autophagy. The interaction between ATG16L1 and the ATP6V1A subunit of V-ATPase is abolished by the K490A mutation on ATG16L1 [15]. Another study reported that ATG16L1 participates in PRR-mediated innate immune signaling pathway and negatively regulates pro-inflammatory and inflammatory responses and IFN- responses mediated by TLRs, NLRs, and RLRs [16]. However, there are few studies on the function and mechanism of fish ATG16L1 in antiviral innate immunity.

As one of the “four famous domestic fishes” in China, black carp (*Mylopharyngodon piceus*) is a crucial freshwater aquaculture fish. However, numerous microbial diseases threaten this economically important species. Our previous studies demonstrated that bcMAVS is an indispensable adaptor protein in RLR signaling in black carp [17–20]. In this report, we cloned the ATG16L1 homolog of black carp (bcATG16L1) and characterized its negative regulatory role in bcMAVS-mediated IFN signaling. Immunofluorescence data identified that bcATG16L1 was primarily a cytosolic protein. Besides, we found that when bcATG16L1 is co-transfected with bcMAVS, it significantly inhibited bcMAVS-mediated IFN signaling and antiviral activity against SVCV.

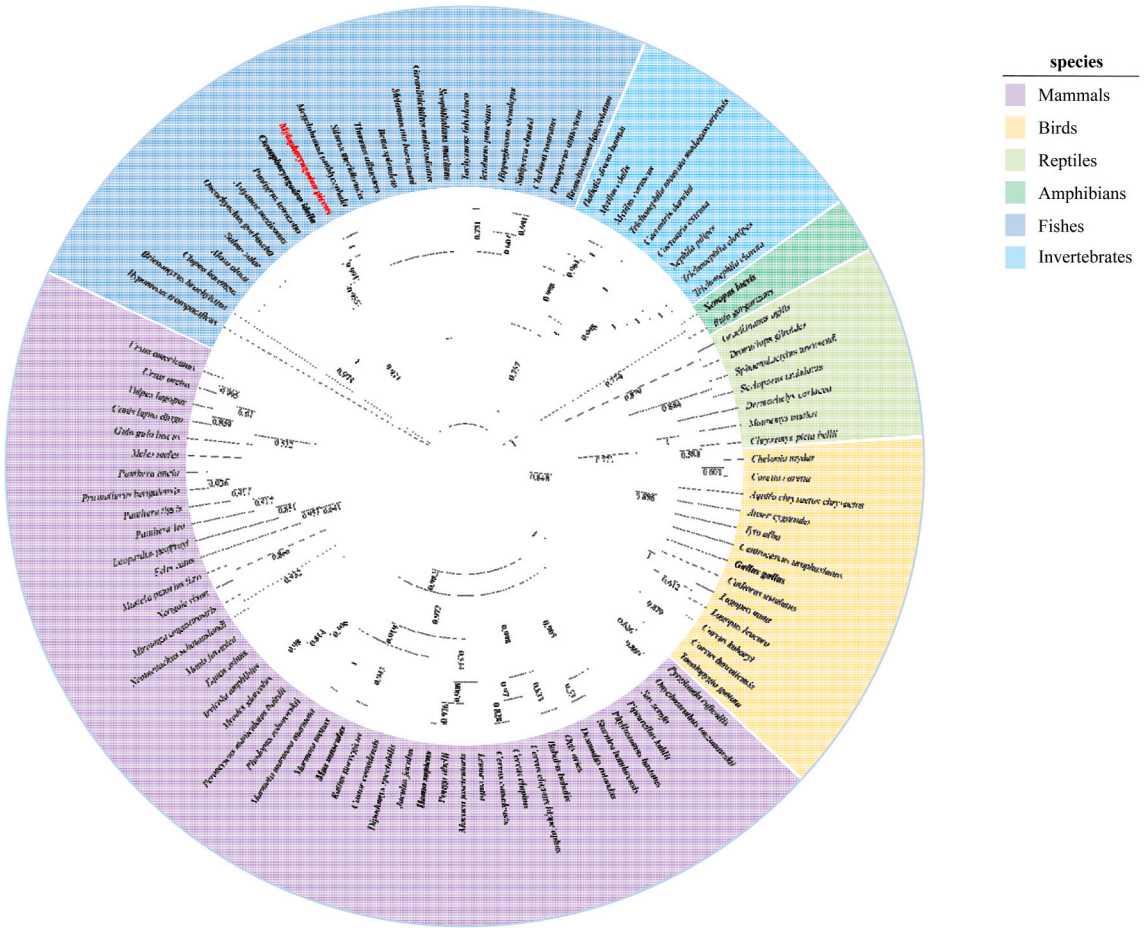

Fig. 2. Evolutionary tree of ATG16L1 homologs.
The phylogenetic trees were constructed by aligning ATG16L1 protein sequences of 100 selected species. This evolutionary tree was created by MEGA-X software and embellished by iTOL (https://itol.embl.de/). Species' Latin names, gene IDs, and corresponding identities are shown in Table 2. Clustal Omega of EMBL-BEI website was used to analyze the identity of ATG16L1 of each species and ATG16L1 of black carp (https://www.ebi.ac.uk/Tools/msa/clustalo/).

Furthermore, we confirmed the interaction between bcATG16L1 and bcMAVS by co-immunoprecipitation assay. Taken together, our data demonstrate that bcATG16L1 is a suppressor in regulating RLR/IFN signaling transduction that targets bcMAVS.

2. Materials and methods

2.1. Cloning of bcATG16L1

The total RNA was extracted from the spleen of black carp by using Trizol (Takara, Japan). Then, first-strand cDNA was obtained by reverse transcription using Revert Aid First Strand cDNA Synthesis Kit (Thermo, USA). The CDS of bcATG16L1 was cloned into the pMD18-T vector (Jakara, Tapara, Japan) by PCR and then verified by DNA sequencing. The primers were listed in Table 1. The recombinant expression vector was constructed by cloning the open reading frame (ORF) region into pcDNA5/FRT/TO-HA vector (Invitrogen, USA) for eukaryotic expression.

2.2. Cells, plasmids, and transfection

Epithelioma papulosum cyprini (EPC), HeLa and human embryonic kidney 293T (HEK293T) cells were cultured in DMEM (Gibco, USA) supplemented with 10% FBS (Gibco, USA); EPC cells were cultured at 26 °C; HeLa and HEK293T cells were cultured at 37 °C. The plasmids used in the luciferase reporter assay such as pcDNA5/FRT/TO, pRL-TK, Luci-DrIFNφ1 (for zebrafish IFNφ1 promoter) and Luci-bcIFNa (for black carp IFNa promoter) were kept in our lab. The transfection reagent for EPC and HEK293T cells was polyetherimide (PEI) (Polysciences, USA), and that for Hela cells was LipoMax (32012, Sudgen).

2.3. Western blot assay

At 48 h post-transfection, cells were washed with phosphate buffer solution (PBS) and prepared by mixing with SDS-PAGE protein loading buffer. Samples were boiled for 15 min, electrophoresed in 10% SDS-polyacrylamide gels, and then transferred to PVDF membrane using Trans-Blot (Bio-Rad). The PVDF membrane was blocked with 5% skim milk, probed with primary antibody, followed by incubation with secondary antibody. Target proteins were visualized with BCIP/NBT alkaline phosphatase color reagent (Sigma, USA).

2.4. Immunofluorescence microscopy

Cells were seeded in 24 well plates. At 24 h post-transfection, cells were fixed with 4% paraformaldehyde for 15 min, penetrated with 0.2% Triton-x-100 for 15 min, and blocked with 10% FBS for 1 h. Then cells were incubated with primary antibodies (anti-Flag or anti-HA) for 1–2 h. Subsequently, the cells were incubated with the second antibody with fluorescence for 1–2 h. Finally, images were obtained with a confocal microscope.

Table 2
Comparison of ATG16L1 homologs of different species.

Species	Accession number	Identity	Species	Accession number	Identity
Mylopharyngodon piceus	OP727268	100	*Ovis aries*	XP_027823279.2	74.58
Megalobrama amblycephala	XP_048015642.1	99.34	*Mirounga angustirostris*	XP_045723665.1	74.58
Ctenopharyngodon idella	QEE80076.1	99.18	*Meles meles*	XP_045874527.1	74.58
Puntigrus tetrazona	XP_043114271.1	94.7	*Gulo gulo luscus*	KAI5770022.1	74.58
Astyanax mexicanus	XP_022526000.2	90.5	*Cervus elaphus*	XP_043732598.1	74.58
Alosa alosa	XP_048120408.1	88.72	*Cervus canadensis*	XP_043317953.1	74.58
Clupea harengus	XP_012693380.1	88.41	*Neomonachus schauinslandi*	XP_021534705.1	74.42
Tachysurus fulvidraco	XP_026994591.1	88.26	*Neogale vison*	XP_044097810.1	74.42
Siniperca chuatsi	XP_044057348.1	87.42	*Macaca fascicularis*	XP_005574704.1	74.42
Oncorhynchus gorbuscha	XP_046150979.1	87.11	*Jaculus jaculus*	XP_004662320.1	74.42
Salmo salar	XP_014015452.1	86.92	*Equus asinus*	XP_014718034.1	74.42
Hypomesus transpacificus	XP_046891070.1	86.9	*Ursus arctos*	XP_026347454.1	74.25
Thunnus albacares	XP_044209701.1	86.59	*Ursus americanus*	XP_045650053.1	74.25
Betta splendens	XP_029026191.1	86.59	*Prionailurus bengalensis*	XP_043434137.1	74.25
Silurus meridionalis	XP_046718210.1	85.95	*Panthera uncia*	XP_049470612.1	74.25
Hippoglossus stenolepis	XP_035010361.1	85.69	*Panthera tigris*	XP_042851642.1	74.25
Ictalurus punctatus	XP_017346035.1	85.45	*Panthera leo*	XP_042806509.1	74.25
Melanotaenia boesemani	XP_041850156.1	85.07	*Mustela putorius furo*	XP_004773562.1	74.25
Scophthalmus maximus	XP_035477803.1	83.94	*Leopardus geoffroyi*	XP_045337718.1	74.25
Girardinichthys multiradiatus	XP_047248337.1	83.69	*Lemur catta*	XP_045415559.1	74.25
Chelmon rostratus	XP_041795991.1	83.14	*Desmodus rotundus*	XP_024419640.1	74.25
Brienomyrus brachyistius	XP_048845584.1	82.75	*Felis catus*	XP_023115588.1	74.09
Cervus elaphus hippelaphus	OWK05108.1	76.82	*Vulpes lagopus*	XP_041622588.1	73.96
Taeniopygia guttata	XP_012431023.1	76.58	*Canis lupus dingo*	XP_025319265.2	73.96
Catharus ustulatus	XP_032924212.1	76.58	*Homo sapiens*	NP_060444.3	73.76
Tyto alba	XP_032846487.1	76.41	*Sturnira hondurensis*	XP_036919381.1	73.75
Onychostruthus taczanowskii	XP_041270326.1	76.41	*Pongo abelii*	NP_001125757.1	73.75
Mauremys mutica	XP_044887032.1	76.41	*Phodopus roborovskii*	CAH6791901.1	73.75
Corvus kubaryi	XP_041876624.1	76.41	*Mus musculus*	NP_001192320.1	73.63
Corvus hawaiiensis	XP_048169791.1	76.41	*Castor canadensis*	JAV38215.1	73.63
Aquila chrysaetos chrysaetos	XP_029883381.1	76.41	*Marmota monax*	XP_046295704.1	73.59
Gallus gallus	XP_004936995.1	76.29	*Pipistrellus kuhlii*	XP_036277225.1	73.42
Lagopus muta	XP_048810885.1	76.25	*Peromyscus maniculatus bairdii*	XP_006984298.1	73.42
Lagopus leucura	XP_042741276.1	76.25	*Myodes glareolus*	XP_048284854.1	73.42
Dermochelys coriacea	XP_038271698.1	76.25	*Marmota marmota marmota*	XP_015337068.1	73.42
Chelonia mydas	XP_007052653.1	76.25	*Dipodomys spectabilis*	XP_042534993.1	73.42
Centrocercus urophasianus	XP_042676585.1	76.25	*Arvicola amphibius*	XP_038194732.1	73.42
Anser cygnoides	XP_047919103.1	76.25	*Protopterus annectens*	XP_043926519.1	73.26
Chrysemys picta bellii	XP_023967232.1	76.15	*Rattus norvegicus*	NP_001102279.2	73.09
Caretta caretta	XP_048720019.1	76.08	*Xenopus laevis*	XP_018119680.1	72.64
Pyrgilauda ruficollis	XP_041323455.1	75.99	*Haliotis discus hannai*	UVK71169.1	50.28
Dromiciops gliroides	XP_043857990.1	75.79	*Branchiostoma lanceolatum*	CAH1245036.1	48.59
Gracilinanus agilis	XP_044529240.1	75.42	*Mytilus coruscus*	CAC5386931.1	47.06
Sphaerodactylus townsendi	XP_048361354.1	75.25	*Mytilus edulis*	CAG2223828.1	45.92
Bufo gargarizans	XP_044145022.1	75.04	*Trichonephila inaurata madagascariensis*	GFS35448.1	44.73
Sus scrofa	ADH81744.1	74.75	*Caerostris darwini*	GIY50131.1	42.88
Sceloporus undulatus	XP_042313615.1	74.75	*Nephila pilipes*	GFT53611.1	31.13
Bubalus bubalis	XP_006041818.2	74.75	*Trichonephila clavipes*	GFU96415.1	30.68
Manis javanica	KAI5930504.1	74.63	*Trichonephila clavata*	GFQ66404.1	29.66
Phyllostomus hastatus	XP_045701677.1	74.58	*Caerostris extrusa*	GIY91549.1	29.64

2.5. Luciferase reporter assay

pcDNA5/FRT/TO-bcATG16L1, pRL-TK (25ng/well) and Luci-bcIFNa (or Luci-DrIFNφ1) (250ng/well) were co-transfected into EPC cells. The cells were harvested 24 h post-transfection and assayed according to the instructions of the luciferase reporter assay system kit (Promega, USA). Briefly, cells were lysed with passive lysis buffer (PLB, Promega, USA) for 15 min and then added into the 96-well plate for measuring luciferase activity according to the manufacturer's instructions. Firefly luciferase activity was normalized based on Renilla luciferase activity.

2.6. Co-immunoprecipitation (Co-IP)

Cells were harvested 48 h post-transfection and lysed in 1 ml 1% NP40 buffer containing 10 μl protease inhibitor cock tail (Bimake. USA), then breaking cells with an ultrasonic crusher. The cellular debris was removed after centrifugation, then the remaining lysate was incubated with protein A/G for 2 h (4 °C) to remove the non-specifically interaction protein. Subsequently, the lysate was incubated with anti-tag-conjugated protein A/G agarose beads (Sigma, USA) overnight (4 °C). Immunoprecipitated proteins were washed 6 times with 1% NP40 buffer and used for IB assay.

2.7. Viruses production and titration

In EPC cells, SVCV (strain: SVCV 741) was propagated in DMEM supplemented with 2% FBS at 26 °C. Plaque assay was used to determine the virus titer on EPC cells. In a nutshell, EPC cells in a 24-well plate were exposed to a 10-fold serially diluted viral supernatant and incubated at 26 °C for 2 h. The supernatant was replaced with fresh DMEM containing 2% FBS and 0.75% methylcellulose after incubation (Sigma). On the third day following the infection, plaques were counted to calculate the virus titer.

2.8. Statistics analysis

Data from viral titer measurement and luciferase reporter assay were obtained from three independent experiments. Error bars represent the

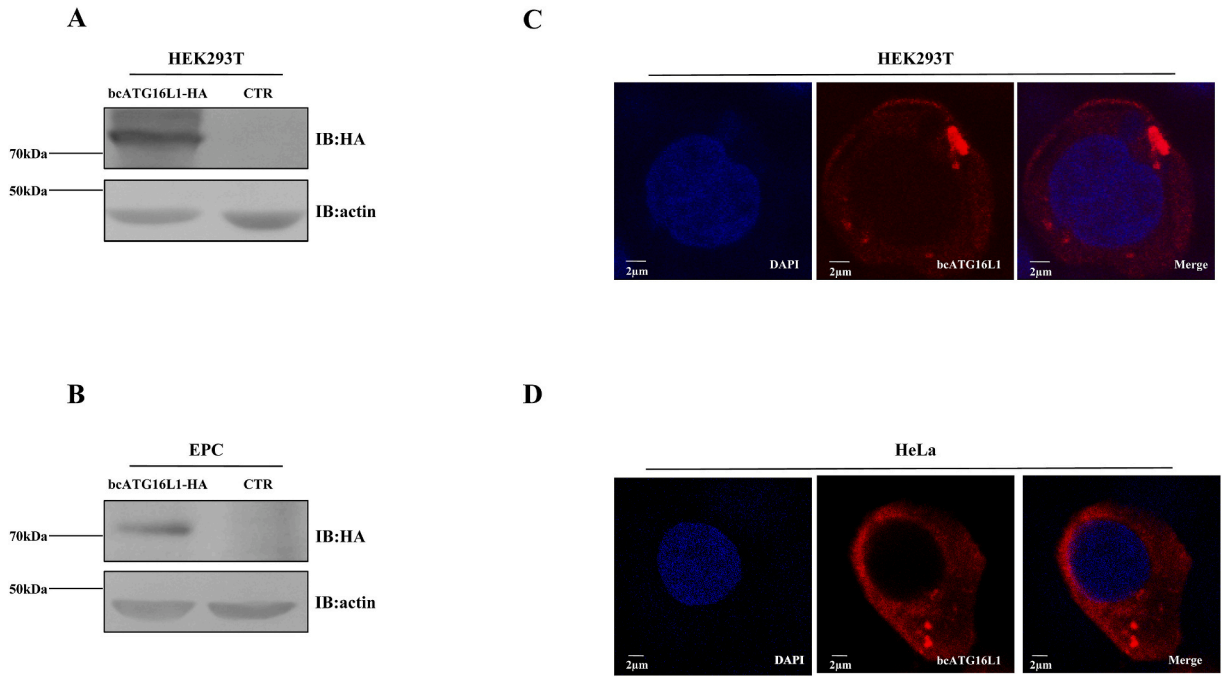

Fig. 3. Protein expression and subcellular localization of bcATG16L1.
(A&B) HEK293T cells (A) or EPC cells (B) were transfected with pcDNA5/FRT-TO/bcATG16L1-HA or pcDNA5/FRT-TO/HA, respectively. The transfected cells were harvested at 48 h post-transfection and the expression of bcATG16L1 was detected by immunoblotting assay. (C&D) HEK293T cells (C) or HeLa cells (D) were transfected with pcDNA5/FRT/TO-bcATG16L1-HA (500 ng/well). At 24 h post-transfection, cells were used for immunofluorescence staining according to the methods. bcATG16L1 was detected by an anti-HA antibody with red fluorescence, nucleus were stained with DAPI. The bars stand for the scale of 10 μm as shown in the pictures. bcATG16L1: pcDNA5/FRT/TO-bcATG16L1-HA.

standard error of the mean value (+SEM) of three independent experiments. Two-tailed Student's t-test was used to analyze the data. Data with a p-value of less than 0.05 were considered statistically significant (*$p < 0.05$; **$p < 0.01$). Two groups with no significant difference ($p < 0.05$) were marked with the same letter.

3. Results

3.1. Bioinformatics analysis of ATG16L1 sequences

The sequence results showed that bcATG16L1 (NCBI accession number: OP727268) was composed of 1830 nucleotides and encoded 609 amino acids. To investigate the conservation of ATG16L1 in vertebrates, the amino acid sequences of ATG16L1 from *Homo sapiens, Mus musculus, Gallus gallus, Xenopus laevis, Ctenopharyngodon idella*, and *Mylopharyngodon piceus* were aligned. We used MEGA-X for Cluster-W analysis and then used Gene-Doc software to complete the layout. The results suggest that ATG16L1 is highly conserved from fish to mammals, except for a few short, low-complexity regions in the middle (Fig. 1A). From the N-terminal to the C-terminal, bcATG16L1 is mainly composed of a coiled-coil domain (76-227aa) and seven WD40 domains (313-352aa, 357-396aa, 399-438aa, 441-477aa, 480-518aa, 521-564aa, and 567-607aa) (Fig. 1B). 3-dimensional structures of ATG16L1 protein in *Mylopharyngodon piceus* and *Homo sapiens* were predicted by AlphaFold 2. Corresponding to the colors in Fig. 1B, we used PyMOL software to highlight the coiled-coil domains (blue), low-complexity domains (purple), and WD40 domains (green). As shown in Fig. 1C, the ATG16L1 protein of human and black carp are highly similar in the tertiary structure, especially, in their coiled-coil domains and WD40 domains.

3.2. The evolutionary tree of ATG16L1

To further investigate the evolutionary origin of ATG16L1, we performed phylogenetic tree analyses using ATG16L1 homologous sequences from 100 species including mammals (45 species), birds (13 species), reptiles (7 species), amphibians (2 species), fish (24 species), and invertebrate (9 species). Although most of the 100 species were randomly selected, they still showed more than 50% of the bootstraps value for each other. The ATG16L1 homologous sequences of *Mylopharyngodon piceus* and *Megalobrama amblycephala* converged in the same branch which is close to *Ctenopharyngodon idella*, indicating that ATG16L1 is highly similar in Cyprinidae (Fig. 2). In addition, we compared the identity of amino acid sequences of ATG16L1 between black carp and other species. The results showed that the sequence identity of more than 90% of selected species was higher than 70%, indicating that ATG16L1 is highly conserved in evolution (Table 2).

3.3. Protein expression and subcellular localization of bcATG16L1

To investigate the protein expression of bcATG16L1, lysates of HEK293T or EPC cells transfected with pcDNA5/FRT/TO-bcATG16L1-HA plasmid were subjected to immunoblotting (IB) assay. In the whole cell lysates of HEK293T and EPC cells expressing bcATG16L1, anti-HA antibodies detected a clear band of approximately 74 kDa migration (Fig. 3A&B). Western blot results showed that bcATG16L1 protein was correctly expressed in both mammalian and fish cells.

To further determine the intracellular localization of bcATG16L1, plasmids encoding bcATG16L1 were transfected into HEK293T cells and HeLa cells, respectively, and these cells were used for IF assay. Confocal fluorescence microscopy showed that bcATG16L1 protein (red) was distributed in the cytoplasm, but not in the nucleus, indicating that bcATG16L1 was mainly a cytosolic protein. It is noteworthy that there were brilliant red dots distributed in the bcATG16L1-expressing region. We speculated that these dots might be aggregates formed by bcATG16L1 itself or autophagy-related vesicles formed by bcATG16L1 together with other autophagy-related proteins (Fig. 3C&D).

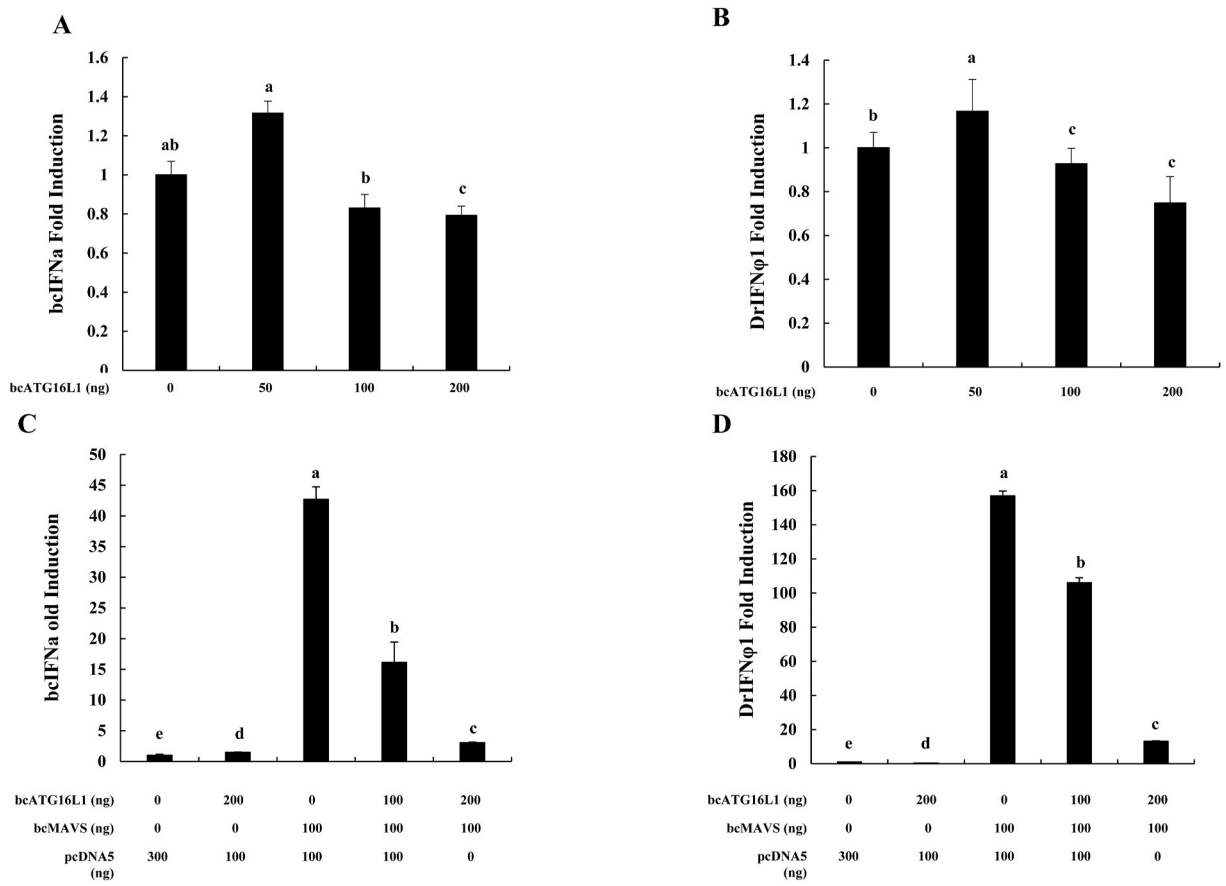

Fig. 4. bcATG16L1 suppressed bcMAVS-mediated IFN promoter activation.
EPC cells in 24-well plates were transfected with pcDNA5/FRTTO-bcATG16L1-HA (0 ng, 50 ng, 100 ng, or 200 ng/well), pRL-TK and Luci-bcIFNa (A), or Luci-DrIFNφ1 (B). At 24 h post-transfection, the promoter activity was detected by luciferase reporter assay. (C&D) EPC cells in 24-well plates were co-transfected with plasmids expressing bcATG16L1 and bcMAVS, together with pRL-TK and Luci-bcIFNa (C), or Luci-DrIFNφ1 (D), and used for report assay. bcATG16L1: pcDNA5/FRT/TO-bcATG16L1-HA; bcMAVS: pcDNA5/FRT/TO-Flag-bcMAVS; pcDNA5: pcDNA5/FRTTO.

3.4. bcATG16L1 suppressed bcMAVS-mediated IFN signaling

To investigate the role of bcATG16L1 in IFN signaling, we test the impact of bcATG16L1 on the activation of bcIFNa and DrIFNφ1 promoters through luciferase reporter assay. The results showed that transfection of ATG16L1 alone slightly inhibited IFN promoter transcription (Fig. 4A&B). However, when bcATG16L1 and bcMAVS were co-transfected, the activation of bcIFNa and DrIFNφ1 promoters mediated by bcMAVS was observably and dose-dependently blocked by bcATG16L1 (Fig. 4C&D). These data demonstrated that bcATG16L1 negatively regulates bcMAVS-mediated IFN signaling.

3.5. bcATG16L1 interacted with bcMAVS

To further analyze the relationship between bcATG16L1 and bcMAVS, we performed a co-immunoprecipitation assay. According to the results, the band of bcATG16L1-HA was detected in the protein precipitated by Flag-bcMAVS, indicating that bcATG16L1 could interact with bcMAVS (Fig. 5A). In addition, we co-transfected the expression vectors encoding bcATG16L1 and bcMAVS into HeLa cells, and then performed the immunofluorescence (IF) assay to determine the distribution of bcATG16L1 and bcMAVS. The IF results showed that the bcATG16L1 distribution region (red) overlapped with the bcMAVS distribution region (green) (Fig. 5B).

3.6. bcATG16L1 inhibited the antiviral ability of bcMAVS against SVCV

To evaluate the role of bcATG16L1 in regulating bcMAVS-mediated antiviral activity, EPC cells expressing bcATG16L1 and/or bcMAVS were infected with SVCV at 0.01MOI (multiplicity of infection), 0.1 MOI, and 1MOI, respectively. Then the supernatant was used for plaque assay to determine the viral titer. The viral titers in the supernatants of EPC cells expressing bcMAVS alone were significantly lower than those of control cells, whereas the viral titers in the supernatants of cells expressing bcATG16L1 were not significantly different from those of control cells. However, when bcATG16L1 was co-transfected with bcMAVS, bcATG16L1 significantly attenuated bcMAVS-mediated antiviral activity (Fig. 6A). Corresponding to the virus titer assay, crystal violet assay results showed that the cytopathic effects (CPEs) of EPC cells co-transfected with bcATG16L1 and bcMAVS were significantly stronger than those of bcMAVS transfected alone (Fig. 6B). Furthermore, the mRNA levels of SVCV-related genes were detected by the q-PCR assay. Compared with the group in which bcMAVS was transfected alone, the mRNA levels of SVCV-M, SVCV-N, SVCV-P, and SVCV-G in the co-transfected group of bcATG16L1 and bcMAVS were considerably higher (Fig. 6C,F). Taken together, it was concluded that bcATG16L1 can block bcMAVS-mediated antiviral activity.

4. Discussion

In this study, we cloned the ATG16L1 homolog of black carp (bcATG16L1) and compared the sequence of bcATG16L1 with those of

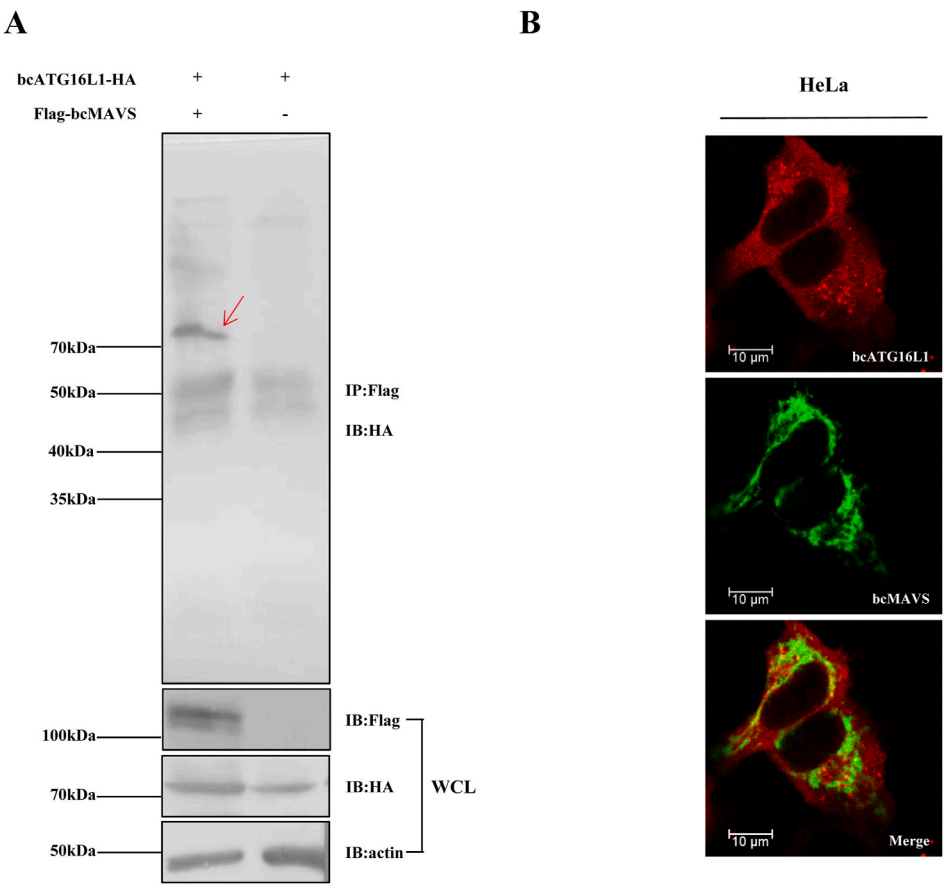

Fig. 5. Protein interaction and subcellular co-localization of bcATG16L1 and bcMAVS.
(A) HEK293T cells in a 10 cm dish were transfected with pcDNA5/FRT/TO-bcATG16L1-HA together with pcDNA5/FRT/TO or pcDNA5/FRT/TO/Flag-bcMAVS. The cells were harvested 48 h post-transfection and used for IP assay. IB: immunoblot; IP: immunoprecipitation; WCL: whole cell lysate. (B) HeLa cells were transfected with pcDNA5/FRT/TO/bcATG16L1-HA (500 ng/well), pcDNA5/FRT/TO-Flag-bcMAVS (500 ng/well), or the empty vector pcDNA5/FRTTO separately. Cells were used for IF staining at 24 hpt.

other species. Amino acid sequence analysis and comparison of ATG16L1 of different species showed that bcATG16L1 was highly identical with ATG16L1 from higher vertebrates. Besides, the protein structure of bcATG16L1 was similar to that of human ATG16L1, which implies that ATG16L1 might also be a protein with evolutionary conservation in function from fish to higher vertebrates. A study using genomic data from American alligator also helps to support this viewpoint, which indicates that autophagy proteins, including ATG16L1, are highly conserved [21].

In mammals, ATG16L1 is an autophagy protein, but accumulating evidence has shown that ATG16L1 also serves non-autophagic functions, such as regulating innate immune signals. For example, ATG16L1 is necessary for the regulation of viral replication through unidentified autophagy-independent mechanisms in the absence of IFN-α/β [22]; colonic tissue deficient in ATG16L1 has increased type I and type II IFN-related gene expression, including Mx [23]; ATG16L1 T300A is related with enhanced IFN-I activity in stage I adenocarcinoma and improved survival and decreased metastasis in human CRC [24]. However, the functional role of fish ATG16L1 in regulating innate immunity needs to be further characterized.

In the present study, to investigate the role of bcATG16L1 in host antiviral immune response, we first examined the induction activity of bcATG16L1 on IFN promoters by using luciferase reporter assays. The results show that over-expression of bcATG16L1 alone in EPC cells slightly inhibited the activation of the DrIFNφ1 or bcIFNa promoters, but it does not do so in a dose-dependent manner. At the transfection dose of 50 ng, bcATG16L1 slightly upregulated interferon expression (Fig. 4A&B). However, when it was co-transfected with bcMAVS, bcATG16L1 inhibited the activation of the interferon promoters mediated by bcMAVS in a dose-dependent manner, which is consistent with the investigation on human ATG16L1. Thus, we inferred that bcATG16L1 might serve as a suppressor in the bcMAVS-dependent signaling pathway and maintain cell homeostasis in uninfected cells.

To further confirm it, we employed a co-IP assay and verified the interaction between bcATG16L1 and bcMAVS (Fig. 5A). As showed in the antiviral experiments, the viral load and viral replication level in bcATG16L1 and bcMAVS co-transfection group were significantly higher than those in bcMAVS single expression group, which further support that bcATG16L1 is an inhibitor in bcMAVS-mediated antiviral immune response.

Similar to our observation in the SVCV infection experiments (Fig. 6C,F), a previous study in *Epinephelus coioides* has found that overexpression of ATG16L1 can promote the replication of SGIV and RGNNV [25]. However, another study has shown that autophagy activated by rapamycin or overexpression of LC3 reduces SGIV replication [26]. These studies suggest that the type of virus and the way autophagy is activated may influence viral replication in a negative or positive way by virtue of the immune function of autophagy proteins. Therefore, the specific regulatory mechanism of ATG16L1 on virus replication remains to be further studied.

Due to MAVS being the core adaptor in the RLR signaling pathway, its activity should be precisely controlled, such as by post-translational modifications or interaction with other regulatory proteins. For instance, many proteins, such as TRIM31, Smurf1, and USP18, are responsible for K63-, K27-, and K48-linked polyubiquitination of MAVS [27]. Our earlier research has uncovered a number of antagonistic regulators that target bcMAVS. While, in this study, the molecular mechanism of bcATG16L1 negatively regulating bcMAVS remains to be further investigated. A study on human ATG16L1 has mentioned that ATG16L1 might control the expression of RIG-I and MDA5 and prevent these proteins from *trans*-locating to the mitochondrial compartment to activate downstream MAVS signaling [24]. Another study has found that ATG16L1 can inhibit RIPK2 polyubiquitination and thus inhibit TLR2-mediated NF-κB activation and pro-inflammatory cytokine

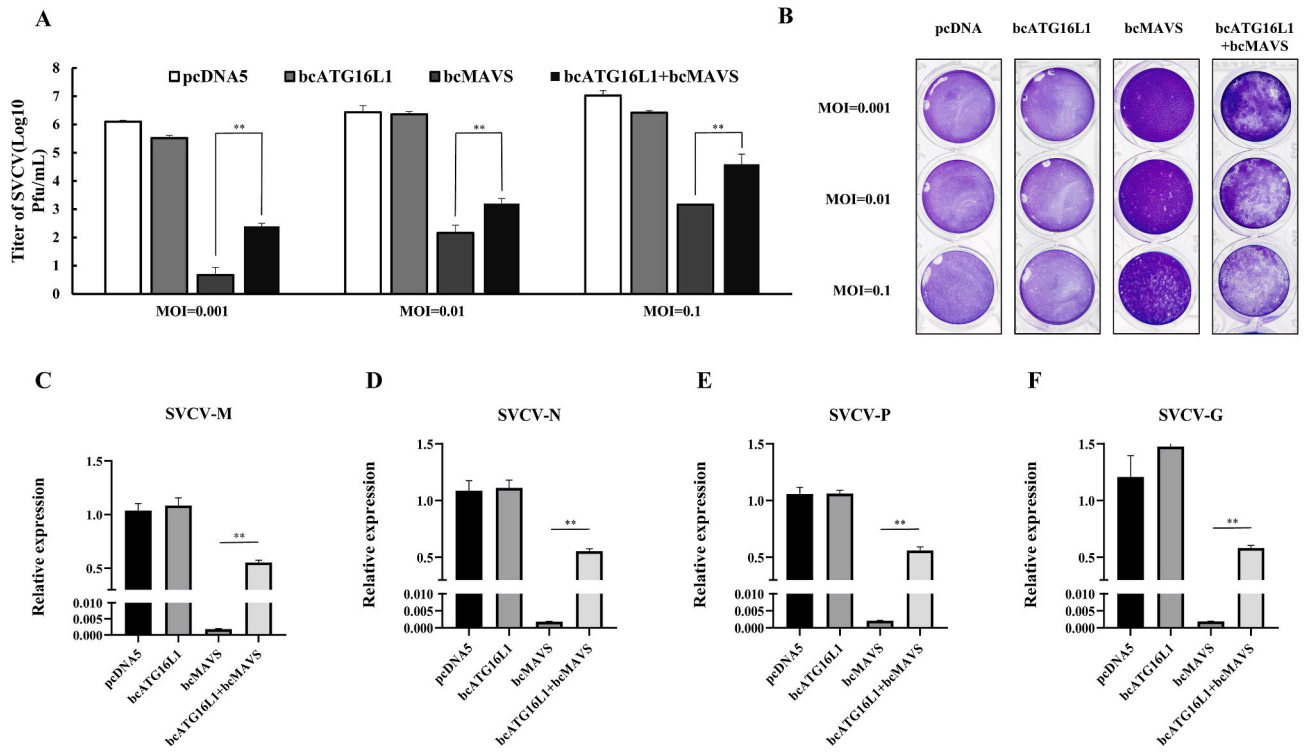

Fig. 6. bcATG16L1 down-regulates the antiviral ability of bcMAVS.
EPC cells in a 24-well plate were transfected with plasmids expressing bcATG16L1 and/or bcMAVS. After 24 h, cells were infected with SVCV at the indicated multiplicity of infection (MOI). (A) The supernatant media were collected at 24 h post-infection and applied for virus titer detection by plaque assay. (B) The cell monolayers were stained with crystal violet. (C–F) mRNA levels of SVCV-related genes were detected by q-PCR (MOI = 0.1). bcATG16L1: pcDNA5/FRT/TO-bcATG16L1-HA; bcMAVS: pcDNA5/FRT/TO-Flag-bcMAVS; pcDNA5: pcDNA5/FRTTO (as control). Two groups with no significant difference ($p < 0.05$) were marked with the same letter.

production [28]. This suggests that bcATG16L1 may also inhibit the antiviral innate immune activity of bcMAVS through posttranslational modifications such as ubiquitination. The above studies may provide clues for us to further investigate the molecular mechanism of bcATG16L1 regulating bcMAVS.

CRediT authorship contribution statement

Yunfan He: Investigation, Writing – original draft. **Yuqing Peng:** Investigation, Writing – original draft. **Xiaoyu Liu:** Investigation, Formal analysis. **Jiamin Yu:** Investigation, Formal analysis. **Yuting Du:** Investigation, Formal analysis. **Zhiming Li:** Investigation, Formal analysis. **Hui Wu:** Data curation. **Jun Xiao:** Writing – review & editing, Resources. **Hao Feng:** Supervision, Conceptualization, Formal analysis, Project administration.

Data availability

Data will be made available on request.

Acknowledgements

This work was supported the National Natural Science Foundation of China (U21A20268,31920103016, U22A20535, 32173010, 32002415, 32002383), Hunan Provincial Science and Technology Department (2021NK2025, 2022JJ30383), the Modern Agricultural Industry Program of Hunan Province, Hunan Provincial Education Department (20A317), the Research and Development Platform of Fish Disease and Vaccine for Postgraduates in Hunan Province, Hunan province college students research learning and innovative experiment project (S202210542066, S202210542155), college students research learning and innovative experiment project of Hunan Normal University (2022131, 2022272).

References

[1] C. Richetta, M. Faure, Autophagy in antiviral innate immunity, Cell Microbiol. 15 (2013) 368–376, https://doi.org/10.1111/cmi.12043.
[2] K. Onoguchi, M. Yoneyama, T. Fujita, Retinoic acid-inducible gene-I-like receptors, J. Interferon Cytokine Res. 31 (2011) 27–31, https://doi.org/10.1089/jir.2010.0057.
[3] T. Kawai, K. Takahashi, S. Sato, C. Coban, H. Kumar, H. Kato, K.J. Ishii, O. Takeuchi, S. Akira, IPS-1, an adaptor triggering RIG-I- and Mda5-mediated type I interferon induction, Nat. Immunol. 6 (2005) 981–988, https://doi.org/10.1038/ni1243.
[4] J. Xiao, C. Yan, W. Zhou, J. Li, H. Wu, T. Chen, H. Feng, CARD and TM of MAVS of black carp play the key role in its self-association and antiviral ability, Fish Shellfish Immunol. 63 (2017) 261–269, https://doi.org/10.1016/j.fsi.2017.02.023.
[5] A. Meléndez, Z. Tallóczy, M. Seaman, E.-L. Eskelinen, D.H. Hall, B. Levine, Autophagy genes are essential for dauer development and life-span extension in C. elegans, Science 301 (2003) 1387–1391, https://doi.org/10.1126/science.1087782.
[6] E.S. Hars, H. Qi, A.G. Ryazanov, S. Jin, L. Cai, C. Hu, L.F. Liu, Autophagy regulates ageing in C. elegans, Autophagy 3 (2007) 93–95, https://doi.org/10.4161/auto.3636.
[7] M.L. Tóth, T. Sigmond, E. Borsos, J. Barna, P. Erdélyi, K. Takács-Vellai, L. Orosz, A. L. Kovács, G. Csikós, M. Sass, T. Vellai, Longevity pathways converge on autophagy genes to regulate life span in Caenorhabditis elegans, Autophagy 4 (2008) 330–338, https://doi.org/10.4161/auto.5618.
[8] B. Boland, W.H. Yu, O. Corti, B. Mollereau, A. Henriques, E. Bezard, G.M. Pastores, D.C. Rubinsztein, R.A. Nixon, M.R. Duchen, G.R. Mallucci, G. Kroemer, B. Levine, E.-L. Eskelinen, F. Mochel, M. Spedding, C. Louis, O.R. Martin, M.J. Millan, Promoting the clearance of neurotoxic proteins in neurodegenerative disorders of ageing, Nat. Rev. Drug Discov. 17 (2018) 660–688, https://doi.org/10.1038/nrd.2018.109.
[9] J. Ren, Y. Zhang, Targeting autophagy in aging and aging-related cardiovascular diseases, Trends Pharmacol. Sci. 39 (2018) 1064–1076, https://doi.org/10.1016/j.tips.2018.10.005.

[10] X.H. Liang, S. Jackson, M. Seaman, K. Brown, B. Kempkes, H. Hibshoosh, B. Levine, Induction of autophagy and inhibition of tumorigenesis by beclin 1, Nature 402 (1999) 672–676, https://doi.org/10.1038/45257.
[11] A. Fleming, M. Bourdenx, M. Fujimaki, C. Karabiyik, G.J. Krause, A. Lopez, A. Martín-Segura, C. Puri, A. Scrivo, J. Skidmore, S.M. Son, E. Stamatakou, L. Wrobel, Y. Zhu, A.M. Cuervo, D.C. Rubinsztein, The different autophagy degradation pathways and neurodegeneration, Neuron 110 (2022) 935–966, https://doi.org/10.1016/j.neuron.2022.01.017.
[12] L.J. Dudley, A.G. Cabodevilla, A.N. Makar, M. Sztacho, T. Michelberger, J. A. Marsh, D.R. Houston, S. Martens, X. Jiang, N. Gammoh, Intrinsic lipid binding activity of ATG16L1 supports efficient membrane anchoring and autophagy, EMBO J. 38 (2019), e100554, https://doi.org/10.15252/embj.2018100554.
[13] B. Ravikumar, K. Moreau, D.C. Rubinsztein, Plasma membrane helps autophagosomes grow, Autophagy 6 (2010) 1184–1186, https://doi.org/10.4161/auto.6.8.13428.
[14] K.M. Hooper, E. Jacquin, T. Li, J.M. Goodwin, J.H. Brumell, J. Durgan, O. Florey, V-ATPase is a universal regulator of LC3-associated phagocytosis and non-canonical autophagy, J. Cell Biol. 221 (2022), e202105112, https://doi.org/10.1083/jcb.202105112.
[15] Y. Lei, D.J. Klionsky, The coordination of V-ATPase and ATG16L1 is part of a common mechanism of non-canonical autophagy, Autophagy 18 (10) (2022 Oct) 2267–2269, https://doi.org/10.1080/15548627.2022.2100678. Epub 2022 Jul 19. PMID: 35811564; PMCID: PMC9542863.
[16] D. Hamaoui, A. Subtil, ATG16L1 functions in cell homeostasis beyond autophagy, FEBS J. 289 (2022) 1779–1800, https://doi.org/10.1111/febs.15833.
[17] Y. Cao, Z. Chen, J. Huang, H. Wu, J. Zou, H. Feng, Black carp TUFM collaborates with NLRX1 to inhibit MAVS-mediated antiviral signaling pathway, Dev. Comp. Immunol. 122 (2021), 104134, https://doi.org/10.1016/j.dci.2021.104134.
[18] Z. Chen, Y. Cao, J. Huang, Y. Tan, J. Wei, J. Xiao, J. Zou, H. Feng, NLK suppresses MAVS-mediated signaling in black carp antiviral innate immunity, Dev. Comp. Immunol. 122 (2021), 104105, https://doi.org/10.1016/j.dci.2021.104105.
[19] Y. Dai, Y. Cao, Z. Chen, J. Huang, J. Xiao, J. Zou, H. Feng, RIPK3 collaborates with RIPK1 to inhibit MAVS-mediated signaling during black carp antiviral innate immunity, Fish Shellfish Immunol. 115 (2021) 142–149, https://doi.org/10.1016/j.fsi.2021.06.011.
[20] W. Li, Y. Cao, Z. Chen, Y. Tan, Y. Dai, J. Wei, J. Xiao, H. Feng, Black carp TRADD suppresses MAVS/IFN signaling during the innate immune activation, Fish Shellfish Immunol. 111 (2021) 83–93, https://doi.org/10.1016/j.fsi.2021.01.006.
[21] A. Hale, M. Merchant, M. White, Detection and analysis of autophagy in the American alligator (Alligator mississippiensis), J. Exp. Zool. B Mol. Dev. Evol. 334 (2020) 192–207, https://doi.org/10.1002/jez.b.22936.
[22] S. Hwang, N.S. Maloney, M.W. Bruinsma, G. Goel, E. Duan, L. Zhang, B. Shrestha, M.S. Diamond, A. Dani, S.V. Sosnovtsev, K.Y. Green, C. Lopez-Otin, R.J. Xavier, L. B. Thackray, H.W. Virgin, Nondegradative role of Atg5-Atg12/Atg16L1 autophagy protein complex in antiviral activity of interferon gamma, Cell Host Microbe 11 (2012) 397–409, https://doi.org/10.1016/j.chom.2012.03.002.
[23] A.M. Marchiando, D. Ramanan, Y. Ding, L.E. Gomez, V.M. Hubbard-Lucey, K. Maurer, C. Wang, J.W. Ziel, N. van Rooijen, G. Nuñez, B.B. Finlay, I. U. Mysorekar, K. Cadwell, A deficiency in the autophagy gene Atg16L1 enhances resistance to enteric bacterial infection, Cell Host Microbe 14 (2013) 216–224, https://doi.org/10.1016/j.chom.2013.07.013.
[24] W.A. Grimm, J.S. Messer, S.F. Murphy, T. Nero, J.P. Lodolce, C.R. Weber, M. F. Logsdon, S. Bartulis, B.E. Sylvester, A. Springer, U. Dougherty, T.B. Niewold, S. S. Kupfer, N. Ellis, D. Huo, M. Bissonnette, D.L. Boone, The Thr300Ala variant in ATG16L1 is associated with improved survival in human colorectal cancer and enhanced production of type I interferon, Gut 65 (2016) 456–464, https://doi.org/10.1136/gutjnl-2014-308735.
[25] C. Li, L. Wang, X. Zhang, J. Wei, Q. Qin, Molecular cloning, expression and functional analysis of Atg16L1 from orange-spotted grouper (Epinephelus coioides), Fish Shellfish Immunol. 94 (2019) 113–121, https://doi.org/10.1016/j.fsi.2019.09.004.
[26] C. Li, L. Wang, J. Liu, Y. Yu, Y. Huang, X. Huang, J. Wei, Q. Qin, Singapore Grouper Iridovirus (SGIV) inhibited autophagy for efficient viral replication, Front. Microbiol. 11 (2020) 1446, https://doi.org/10.3389/fmicb.2020.01446.
[27] J. Hou, L. Han, Z. Zhao, H. Liu, L. Zhang, C. Ma, F. Yi, B. Liu, Y. Zheng, C. Gao, USP18 positively regulates innate antiviral immunity by promoting K63-linked polyubiquitination of MAVS, Nat. Commun. 12 (2021) 2970, https://doi.org/10.1038/s41467-021-23219-4.
[28] H. Honjo, T. Watanabe, Y. Arai, K. Kamata, K. Minaga, Y. Komeda, K. Yamashita, M. Kudo, ATG16L1 negatively regulates RICK/RIP2-mediated innate immune responses, Int. Immunol. 33 (2021) 91–105, https://doi.org/10.1093/intimm/dxaa062.